July 19, 1999

# Prediction of linearly polarised Bremsstrahlung Production for ELFE at CERN

**F.A. Natter, P. Grabmayr**

*Physikalisches Institut, Universität Tübingen, Germany*
*on request by HaPHEEP*

## The calculations

At an electron beam energy of 25 GeV the mean opening angle of the photon beam (variance) amounts to 0.02 mrad. Due to this high energy the discontinuity depends very sensitive on the crystal angles $(\theta, \alpha)$ which would have to be aligned to an accuracy less then half a mrad. Similarly stringent requirements apply to the electron beam specifications. In order to minimize the influence of the electron beam divergence and multiple scattering in the target, which depletes the polarisation, a 0.1 mm thick radiator was considered. The desired discontinuity at $k_d = 12$ GeV can be achieved by only a few combinations of crystal angles. The values of tab. 1, were chosen for ease of crystal alignment. Out of a set of 9261 contributing lattice vectors (miller indices $|h_i| \leq 10$) the 100 strongest contributing vectors were used for this calculation. Each other vector contributes less than $10^{-4}$ with respect to the

Table 1: Parameters used for all calculations

| parameter | unit | value(s) | | |
|---|---|---|---|---|
| beam energy | MeV | 25300 | | |
| energy spread | MeV | 20 | | |
| crystal angles $(\theta, \alpha, \Phi)$ | rad | 0.03 | 0.77 | 0.7854 |
| beam divergence | mrad | 0.01 | | |
| beam spot size | mm | 1 | | |
| thickness of radiator | mm | 0.1 | | |
| radiator temperature | K | 293.17 | | |
| Z of radiator (diamond,Ni) | - | 6 | 30 | |

strongest one (here the lattice vector $[02\bar{2}]$) to the cross section. Including all experimental deficiencies (tab. 1), the systematic error of the polarisation prediction is estimated to about 2% absolute.

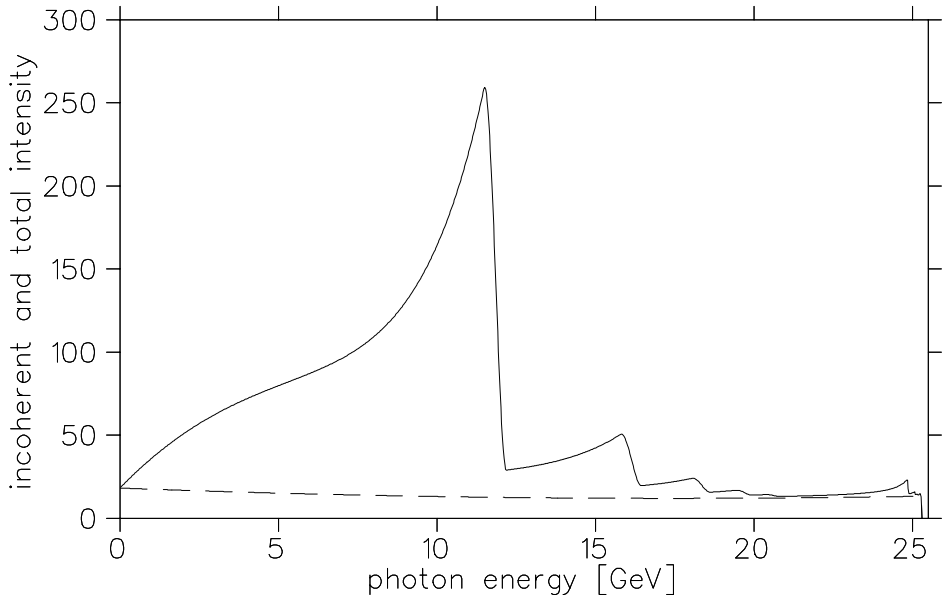


Figure 1: Prediction of total crystal intensity $I^{\mathrm{cry}} = I^{\mathrm{coh}}_{\mathrm{di}} + I^{\mathrm{inc}}_{\mathrm{di}}$ and incoherent $I^{\mathrm{inc}}_{\mathrm{nickel}}$ (dashed) photon intensity using the parameters of tab. 1 and 2, set A.

# Collimation

The angular distribution of the coherent contribution is always narrower than the incoherent one (here $\bar{\vartheta}^{\mathrm{coh}}/\bar{\vartheta}^{\mathrm{inc}} \sim 0.4$). Therefore for an ideal electron beam and a very thin target, the collimation of the photon beam enhances the polarisation whenever the collimation angle is in the order of the mean polar angle of the coherent photon beam. In general experimental deficiencies deplete the maximal photon polarisation. This can be compensated by collimation if the electron divergence and beam spot size is small compared to the collimator angle. In the sense that the area being swept by the photon beam is about the size of the collimator area. For a rough estimate the opening angle of the beam spot viewed from the collimator must be less than half the collimator angle. Therefore an increase of collimator distance

Table 2: Collimation and photon beam properties

| set | beam spot ($\sigma_s$) [mm] | colli/target distance [m] | colli radius | maximal polarisation | tagging efficiency |
|---|---|---|---|---|---|
| A | 1 | 10 | uncoll | .74 | 1 |
| B | 1 | 10 | 0.6 | .75 | .15 |
| C | 1 | 50 | 1.5 | .77 | .30 |
| D | 0.1 | 10 | 1.2 | .78 | .30 |

reduces this opening angle. The parameters given in tab. 1 do not meet the above requirement, because the polar angle distributions of incoherent and coherent contribution have the same widths, hence a collimation is not advisable. Furthermore the sizable electron beam divergence and large beam spot size on the radiator leads to a strongly reduced tagging efficiency, see calculation of set B in tab. 2. Especially the large beam spot size necessitates to place a collimator at least 50 m downstream the radiator for a significant enhancement of the polarisation. The calculations show, that the gain in

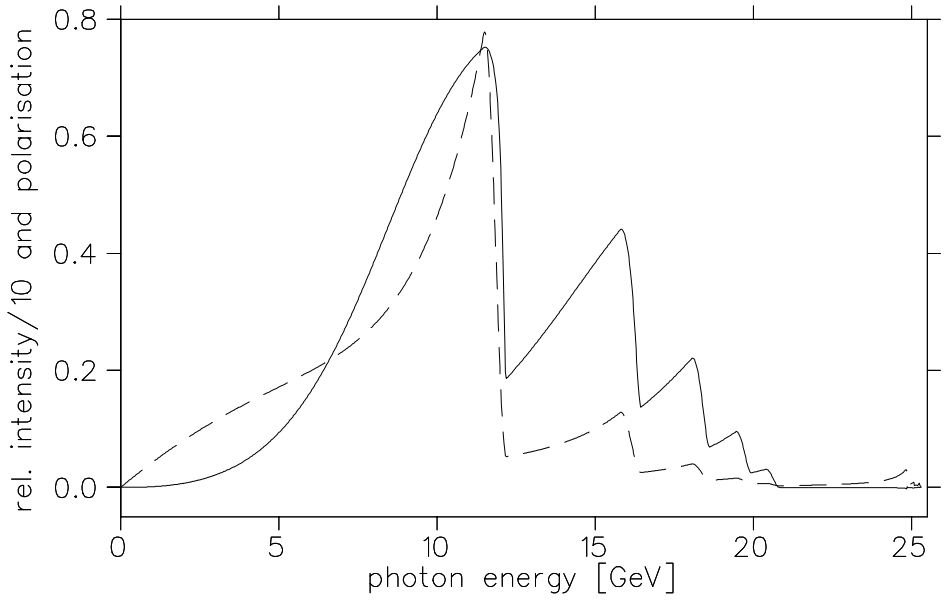


Figure 2: Prediction of relative intensity $I^{\mathrm{rel}} = I^{\mathrm{coh}}_{\mathrm{di}} / I^{\mathrm{inc}}_{\mathrm{nickel}}$ (multiplied by .05, dashed) and photon polarisation without collimation (set A).

polarisation will not balance the smaller photon flux (set C in tab. 2 and fig. 3). A significant reduction of the beam spot size (set D) would be more promising. With very different beam and collimation parameters (set C and D) one can obtain similar cross sections and polarisations.

# Predictions

The calculation simulates the experimental situation, where the crystal intensity is obtained from bremsstrahlung off a diamond radiator. In fig. 1 the absolute intensities from an amorphous (nickel) and a crystal radiator (diamond) are plotted to demonstrate what can be expected from tagging efficiency measurements. The incoherent contribution used for the relative intensity in fig. 2 stems from a nickel radiator in order to allow a comparison to a measured relative intensity. The total crystal intensity is the sum of the coherent and incoherent contribution from diamond, whereas the latter must be distinguished from the incoherent intensity of nickel, which is generally the measured one. From the intensity the cross section per atom is calculated

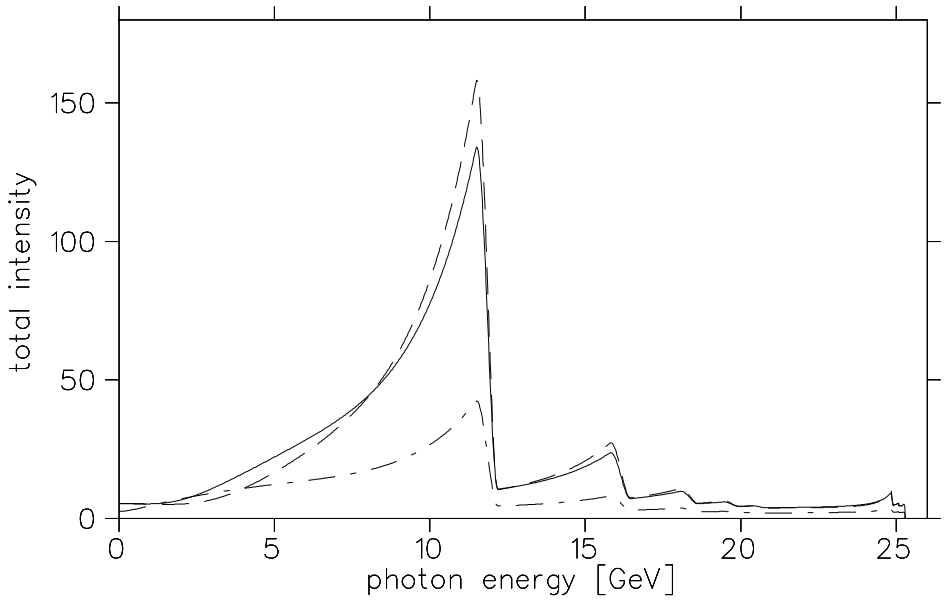


Figure 3: Prediction of abspolute intensity for set B (dot-dashed), C (solid) and D (dashed).

via: $d\sigma/dk = I/k \cdot 20.86$ mbarn, with $k$ being the photon energy. Note that the relative intensity (dashed line in fig. 2) $I^{\mathrm{rel}} = I^{\mathrm{coh}}_{\mathrm{di}}/I^{\mathrm{inc}}_{\mathrm{nickel}}$ is scaled by a factor of 0.05. The linear polarisation is plotted in fig. 2 reaching a maximum polarisation of about $0.7 \pm 0.02$ in the energy region of $11.3 \ldots 11.7$ GeV. On a target, which is for example 10 m afar, 90% of the photon beam would be contained within a circular area of 2.2 mm radius. The results for three sets (B,C,D) of parameters in tab. 2 are shown in figs. 3 and 4.

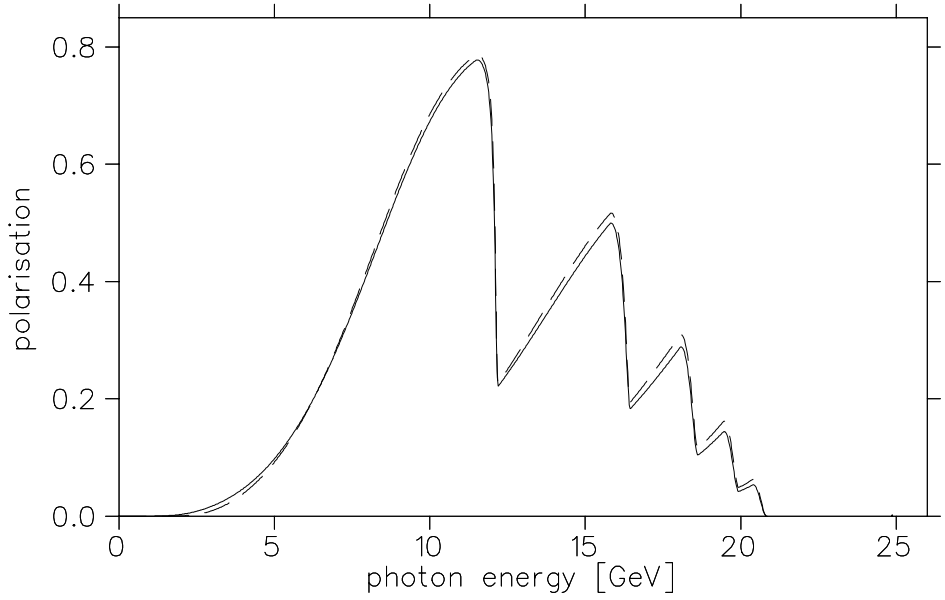


Figure 4: Prediction of polarisation for set C (solid) and set D (dashed). Set B results in similar polarisation than in cases C and D.

# Conclusions

These preliminary calculations show very clearly the importance of good electron beam properties. These should be clarified before further studies as polarisation is rather large in most cases, which is due to the high electron energy favouring coherence effects.

# Photon-flux

The photon flux $d\dot{N}/dk$ is calculated from the intensity $I(k)$ via:

$$\begin{aligned}\frac{d\dot{N}}{dk} &= \frac{J_e}{e}\frac{\rho T N_A}{m_{\mathrm{mol}}^{\mathrm{di}}}\frac{d\sigma}{dk} \\ &= \frac{J_e}{e}\frac{\rho T N_A \bar{\sigma}}{m_{\mathrm{mol}}^{\mathrm{di}}}\frac{I(k)}{k}\end{aligned} \tag{1}$$

Here $J_e/e$ is the electron flux and $\rho$ and $T$ the target density and depth, respectively. $m_{\mathrm{mol}}^{\mathrm{di}}$ denotes the target mass and the cross section unit is given by $\bar{\sigma} = 0.5795 Z^2$ mbarn, whereat $Z_{\mathrm{di}} = 6$. Using the values in tab. 3 for the

Table 3: Constants used for calulating the photonflux

| constant | $\rho$ | $T$ | $m_{\mathrm{mol}}^{\mathrm{di}}$ | $\bar{\sigma}$ |
|---|---|---|---|---|
| unit | [g/cm$^3$] | [cm] | [g/mol] | [cm$^2$] |
| | 3.513 | 0.01 | 12.01 | $2.086 \cdot 10^{-26}$ |

| charge | $J_e$ | $t$ |
|---|---|---|
| unit | [A] | [s] |
| MAMI1 | $3.9 \cdot 10^{-9}$ | 23220 |
| MAMI2 | $5.9 \cdot 10^{-9}$ | 18840 |
| ELFE | $1 \cdot 10^{-4}$ | |

constants in eq. 1 the photonflux is given by $d\dot{N}/dk = 2.3 \cdot 10^{10} \cdot I(k)/k$ and amounts to $3 \ldots 6 \cdot 10^{11}/(\mathrm{GeVs})$ below the discontinuity (12 GeV). In fig. 5 a comparison of the yield from a diamond radiator (set MAMI in tab. 3) with the predicted number of photons per MeV is given. The discrepancy is due to the uncertainty of the measurement of the electron beam current at MAMI. Nevertheless it indicates the reliability of the prediction. The electron beam current of the ELFE scenario is quite high and its an open question which first has to be considered whether the diamond gets heated up too much or suffers radiative damage.

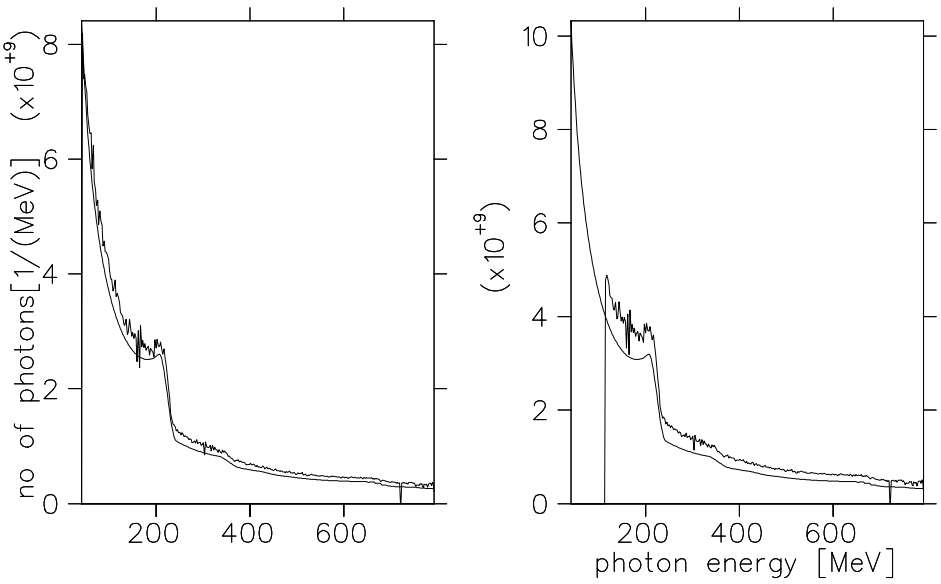


Figure 5: Total number of photons from a beam charge of 387 min · 3.9 nA (MAMI1,*left)* and 314 min · 5.9 nA (MAMI2,*right)*.